Enhanced intensity of global tropical cyclones during the mid-Pliocene warm period

Qing Yan[a,b,1], Ting Wei[c], Robert L. Korty[d], James P. Kossin[e], Zhongshi Zhang[f,g], and Huijun Wang[b]

[a]Nansen-Zhu International Research Centre, Institute of Atmospheric Physics, Chinese Academy of Sciences, Beijing 100029, China; [b]Key Laboratory of Meteorological Disaster/Collaborative Innovation Center on Forecast and Evaluation of Meteorological Disasters, Nanjing University of Information Science and Technology, Nanjing 210044, China; [c]State Key Laboratory of Severe Weather, Chinese Academy of Meteorological Sciences, Beijing 100081, China; [d]Department of Atmospheric Sciences, Texas A&M University, College Station, TX 77843; [e]Center for Weather and Climate, National Oceanic and Atmospheric Administration National Centers for Environmental Information, Madison, WI 53706; [f]Department of Atmospheric Science, School of Environmental Studies, China University of Geosciences, Wuhan 430074, China; and [g]Uni Research Climate, Bjerknes Center for Climate Research, 5007 Bergen, Norway

Edited by Kerry A. Emanuel, Massachusetts Institute of Technology, Cambridge, MA, and approved September 26, 2016 (received for review June 2, 2016)

Given the threats that tropical cyclones (TC) pose to people and infrastructure, there is significant interest in how the climatology of these storms may change with climate. The global historical record has been extensively examined, but it is short and plagued with recurring questions about its homogeneity, limiting its effectiveness at assessing how TCs vary with climate. Past warm intervals provide an opportunity to quantify TC behavior in a warmer-than-present world. Here, we use a TC-resolving (~25 km) global atmospheric model to investigate TC activity during the mid-Pliocene warm period (3.264–3.025 Ma) that shares similarities with projections of future climate. Two experiments, one driven by the reconstructed sea surface temperatures (SSTs) and the other by the SSTs from an ensemble of mid-Pliocene simulations, consistently predict enhanced global-average peak TC intensity during the mid-Pliocene coupled with longer duration, increased power dissipation, and a poleward migration of the location of peak intensity. The simulations are similar to global TC changes observed during recent global warming, as well as those of many future projections, providing a window into the potential TC activity that may be expected in a warmer world. Changes to power dissipation and TC frequency, especially in the Pacific, are sensitive to the different SST patterns, which could affect the viability of the role of TCs as a factor for maintaining a reduced zonal SST gradient during the Pliocene, as recently hypothesized.

mid-Pliocene | tropical cyclone | TC-resolving climate modeling

Tropical cyclones (TCs), one of the most serious natural hazards, pose significant threats to people and infrastructure in coastal regions worldwide. Both theory and modeling studies indicate that mean TC intensity and the frequency of the most intense TCs will likely increase with upward shifts in global temperatures (1–3), and there is evidence for past and projected changes in the latitude of peak TC intensity and TC hazard exposure (4, 5). Studies of how TCs respond to simulations of periods with different climate characteristics in Earth's history may complement these efforts and offer opportunities to better comprehend the processes involved through more varied external forcing.

The mid-Pliocene (3.264–3.025 Ma) represents the most recent period of prolonged global warmth on a geological timescale (6). It features a continental configuration similar to present-day and higher CO_2 levels and arguably provides a potential analog to future greenhouse gas conditions. Benefiting from the Pliocene Research, Interpretation and Synoptic Mapping (PRISM) project (7–10) and Pliocene Model Intercomparison Project (PlioMIP) (11), our knowledge on the thermal structure of the mid-Pliocene ocean is considerably improved. The latest PRISM4 reconstruction (10, 12) indicates stable temperature in the equatorial western Pacific and significant warming in the eastern part during the mid-Pliocene, whereas the PlioMIP models (13) predict higher temperatures (~1–2 °C) over the tropical warm pool relative to the preindustrial, which is supported by the sea surface temperatures (SST) records using the TEX_{86} and corrected Mg/Ca temperature proxies (14, 15). Therefore, it is very interesting to examine how TCs may respond to the two warming scenarios. In addition, whereas it has been argued that global TC activity was greatly enhanced during the early Pliocene (16), which may be important for maintaining a reduced zonal SST gradient over the equatorial Pacific via modulating upper ocean mixing, it remains unclear whether that is also the case for the mid-Pliocene or other plausible SST distributions.

To date, an explicit simulation of TCs during the mid-Pliocene has not yet been performed, although a downscaling method found that storms were stronger and more numerous across the Pacific (16), and the response of environmental conditions important to TC formation in the PlioMIP models has been examined (17). Here we use a TC-permitting (~25 km) global atmospheric circulation model CAM4 (Community Atmospheric Model version 4) to examine characteristics of TC activity during the mid-Pliocene warm period. These results may advance our understanding of future TC behavior and potentially shed light on possible mechanisms responsible for the reduced zonal SST gradient during the mid-Pliocene.

Results

CAM4 explicitly resolves TCs and captures important aspects of their present-day climatological distribution. Based on the tracking algorithm from the Geophysical Fluid Dynamics Laboratory (*Methods*), CAM4 produces an annual number of ~80 TCs with the prescribed modern SST, similar to the estimated TC number (~79) from the International Best Track Archive for Climate Stewardship dataset (1991–2014) (18). The simulated

Significance

To better understand how tropical cyclones (TCs) may respond to future warming, we explore the behavior of TCs during the mid-Pliocene warm period (~3 Ma), which shares characteristics of projected warmer climate. Our TC-permitting numerical simulations predict enhanced global-average peak TC intensity, longer duration, increased power dissipation, and a poleward migration of the location of peak intensity during the mid-Pliocene, although there are regional differences in the magnitude and statistical power of the climate/TC relationships. Our results share similarities with global TC changes observed during recent global warming and in most future projections and provide a window into the potential TC activity that may be expected in a warmer world.

Author contributions: Q.Y. designed research; T.W. performed research; Q.Y. and R.L.K. analyzed data; and Q.Y., R.L.K., J.P.K., Z.Z., and H.W. wrote the paper.

The authors declare no conflict of interest.

This article is a PNAS Direct Submission.

[1]To whom correspondence should be addressed. Email: yanqing@mail.iap.ac.cn.

This article contains supporting information online at www.pnas.org/lookup/suppl/doi:10.1073/pnas.1608950113/-/DCSupplemental.

modern distribution of TCs broadly resembles observations, with the most intense TC activity occurring over the North Pacific (Fig. 1*A* and Fig. S1); and mean TC duration and latitude of the lifetime-maximum windspeed (LMW) is close to observations (Table S1). Note that even at this 25-km resolution, CAM4 is unable to simulate storms of category >3 (Fig. S2), which results in an underestimation of mean TC peak intensity and power dissipation, and CAM4 exhibits weaker TC activity in the North Atlantic than observations.

Driven by the PRISM4 SSTs (Fig. 1*D* and *Methods*), CAM4 predicts a decrease of global-average TC frequency by ∼10% during the mid-Pliocene (Table 1), with a spatial distribution of TCs similar to the preindustrial (Fig. 1*B*). The reduced TC count is more pronounced in the Northern Hemisphere than the Southern Hemisphere (Table 1) and is dominated by negative changes in the occurrence of the weakest storms, while the number of the strongest systems able to be resolved increases (Table S2). The positive contribution to the Northern Hemisphere change mainly comes from the North Pacific, with the negative contribution from the North Atlantic and North Indian Ocean (Fig. 2*A* and Table 1). Meanwhile, global-average LMW is increased during the mid-Pliocene and mean TC duration is longer, leading to more destructive TCs in terms of the power dissipation index (PDI) (19), especially over the Northern Hemisphere (Table 1). This result is in broad agreement with other results that warming might reduce TC genesis, while the number of the most intense events increases (20, 21). Moreover, CAM4 depicts a migration of the location of the peak intensity from the deep tropics during the mid-Pliocene, as well as TC genesis and tracks (Fig. 2 *A* and *C*). The annual mean latitude of peak intensity shifts significantly poleward by ∼2.8° and 3.7° in the Northern and Southern Hemispheres, respectively (Table 1). The poleward trend is observed over each ocean basin, with the largest shift appearing in the western North Pacific and the smallest migration in the North Indian Ocean (which is confined geographically).

In response to the warmer PlioMIP model-based SSTs (Fig. 1*E* and *Methods*), global-average TC frequency exhibit a significant rise by ∼24% (Table 1), with an increase in each TC category (Table S2). Regarding the spatial distribution, this increase is observed mainly over the North Pacific and South Indian Ocean (Fig. 2*B*). The annual mean latitude of peak intensity shows a poleward shift in both hemispheres of ∼1.5°, with positive contributions from all of the ocean basins (Table 1 and Fig. 2*D*). In addition, mean peak intensity is enhanced during the mid-Pliocene, coupled with an increase in the mean duration and PDI of the TCs (Table 1). These features exhibit more hemispheric symmetry than those in response to the PRISM4 SSTs (Table 1).

Although the two mid-Pliocene SST fields result in different response of TC frequency, several common features are observed. Both mid-Pliocene simulations suggest a poleward shift of the location of the LMW over all of the ocean basins, although there are regional differences in the magnitude and statistical power. This result indicates that the migration from the deep tropics is a global phenomenon during the mid-Pliocene, which is similar to the poleward trend in observations from recent decades (5). Next, global-average TCs become stronger during the mid-Pliocene in terms of peak intensity and the number of the most intense storms resolved shows an increase (Table S2), consistent with observed changes during recent warming decades (3). Additionally, global-average TCs tend to be more destructive benefiting from the increased mean TC intensity and duration.

Changes in large-scale environmental conditions play an important role in modulating TC behavior. Major factors controlling TC genesis and intensification include the potential intensity, the moist entropy deficit, and the vertical wind shear (*Methods*). We focus on condition changes over the North Pacific where the most intense changes in peak intensity and poleward migration occur, as well as obvious discrepancy in TC frequency between the two mid-Pliocene simulations. Both mid-Pliocene

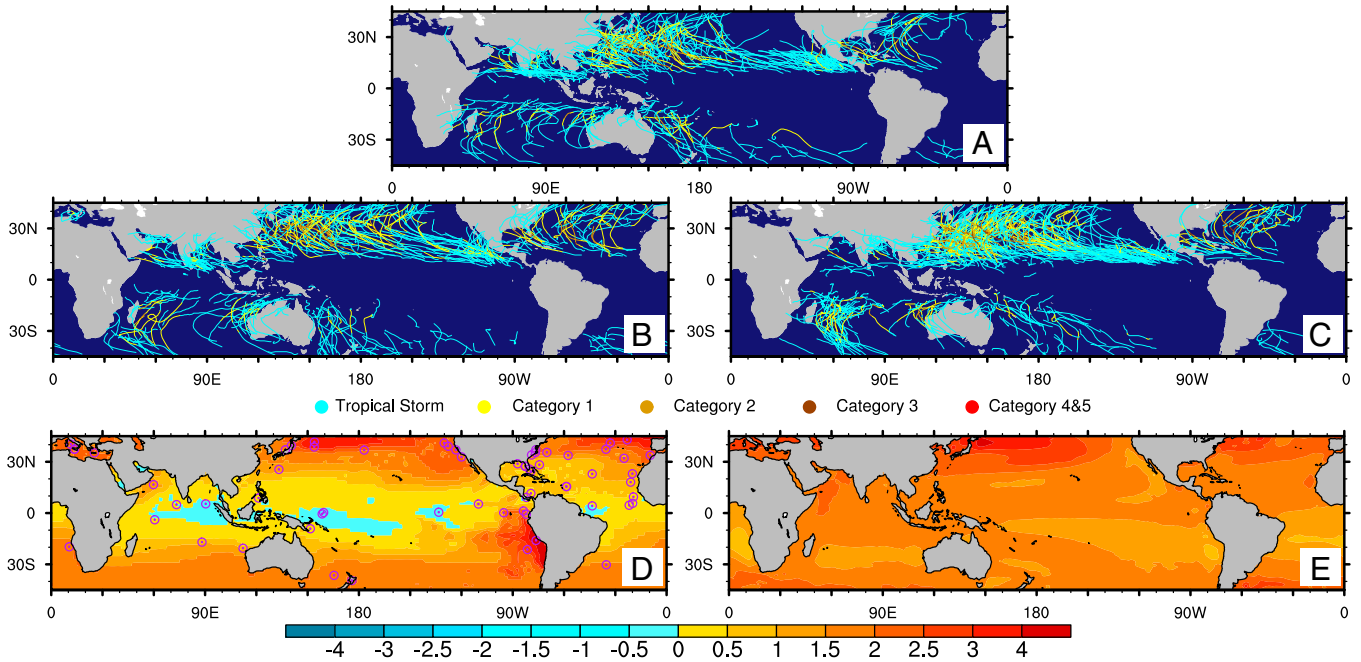

Fig. 1. TC trajectories and mid-Pliocene SST anomalies. TC trajectories in the present-day experiment (*A*) and the mid-Pliocene experiments forced by the PRISM4 SSTs (*B*) and the PlioMIP model-based SSTs (*C*). TC paths are color coded by intensity at each location in their trajectory. The tracks shown in each panel are total TCs in the last 5 y of simulations. Mid-Pliocene SST anomalies (°C) derived from the PRISM4 dataset (*D*) and ensemble mean of the PlioMIP model (*E*). Proxy sites in the PRISM4 dataset are represented by the purple circles in *D*.

Table 1. Changes in mean LMW, duration, PDI, latitude of LMW of a TC, and annual mean TC number between the mid-Pliocene experiment forced by the proxies-based (PlioMIP model-based) SSTs and the preindustrial experiment

Region	LMW, %	Latitude of LMW, °*	Duration, %*	PDI, %	Number, %
Globe[†]	+2.9[#] (+7.1[##])	3.1[##] (1.5[##])	+10.5[#] (+8.8)	+20.8[##] (+35.7[##])	−10.3 (+24.1[##])
NH[§]	+5.7[##] (+7.3[##])	2.8[##] (1.5[##])	+13.9[##] (+8.3)	+28.9[##] (+36.8[##])	−12 (+29.9[##])
SH	−4.5 (+5.8[##])	3.7[##] (1.5)	+1.5 (+9.2)	−3.7 (+25.3[#])	−5.6 (+8.3)
WNP	+10[##] (+9.8[##])	5[##] (1)	+12.3[##] (+2.6)	+43.2[##] (+22)	−40.2[#] (+43.4)
ENP	+7[#] (+5.8)	3.6[##] (1.9[#])	+27.6[#] (+11.7)	+40.9[#] (+42)	−12.9[##] (+46.2[##])
SP	−7.8 (−3.5)	−3.0 (−1.5)	−9.3 (−16.9)	−31.1 (−32.6)	+8 (−6)
NA	+11.1 (+11.2[#])	2.1 (0.8)	+30.7 (+28.6)	+73.3[#] (+101.2[##])	+26.3 (+2.6)
NI	−3.4 (−9.3)	0.1 (1.4)	−6.9 (−28.7)	−17.8 (−30.4)	+42.1[##] (−26.3[#])
SI	−0.7 (+11.9[#])	−3.7[##] (−2.2)	+13.9 (+23.4)	+26.4 (+62.2[##])	−17.2 (+20.7)

*Storms only with the LMW ≥17 m/s are included; duration is defined as the time that a storm spends with intensity ≥17 m/s.

[†]Weighted mean by annual TC number over each ocean basin, also applied for hemispheric average.

[#]Value that passes the 90% significance two-tailed Student *t* test (based on the time series of annual TC metrics in the last 5 y of model simulations).

[##]Value that passes the 95% significance two-tailed Student *t* test (based on the time series of annual TC metrics in the last 5 y of model simulations).

[§]ENP, Eastern North Pacific; NA, North Atlantic; NH, Northern Hemisphere; NI, North Indian Ocean; SH, Southern Hemisphere; SI, South Indian Ocean; SP, South Pacific; WNP, Western North Pacific (Fig. S8).

simulations exhibit greater increase of potential intensity at higher latitudes over the North Pacific (Fig. 3 *A* and *B*) relative to the preindustrial (Fig. S3), indicating a reduced meridional potential intensity gradient in the mid-Pliocene. CAM4 simulates broad regions of decreased moist entropy deficit in the subtropics and increased one in tropical low latitudes (Fig. 3 *C* and *D*), but this pattern is constrained to the eastern North Pacific forced by the PlioMIP SSTs. The reduced meridional gradient in wind shear is also observed in the mid-Pliocene, although wind shear is broadly reduced over the western North Pacific in the simulations with the PRISM4 SSTs (Fig. 3 *E* and *F*). The reduced meridional gradient in environmental conditions, which may be linked with the tropical expansion (i.e., Hadley circulation) in the mid-Pliocene (Fig. S4), indicates increasing favorability for a poleward shift of the latitude of peak intensity in the mid-Pliocene, as well as genesis location and overall storm track. Given broadly reduced wind shear and/or moist entropy deficit in the subtropics, these conditions potentially increase the possibility for a TC to approach its potential intensity and reduce the time required for cyclone genesis and intensification (22), leading to more intense TCs in the mid-Pliocene. At regional scales, the decreased TC genesis over the western North Pacific (~5–25°N) in response to the PRISM4 SSTs results from enhanced moist entropy deficit and slightly decreased potential intensity, whereas the increased TC genesis in response to the PlioMIP model-based SSTs is largely attributed to enhanced potential intensity (Fig. 3).

Discussion

Driven by the PRISM4 and PlioMIP SSTs, our TC-resolving simulations demonstrate that, in a global average, TCs become stronger with longer duration and higher power dissipation in the mid-Pliocene, and the location of peak intensity migrates away from the deep tropics. These metrics are insensitive to the mid-Pliocene SST patterns, although there are regional differences in the magnitude and statistical power. The modeled mid-Pliocene TC characteristics share similarities with the observed TC behavior in recent decades (4, 5, 20, 21), as well as most future projections (1, 3), potentially providing a window into the potential TC activity that may be expected in a warmer world.

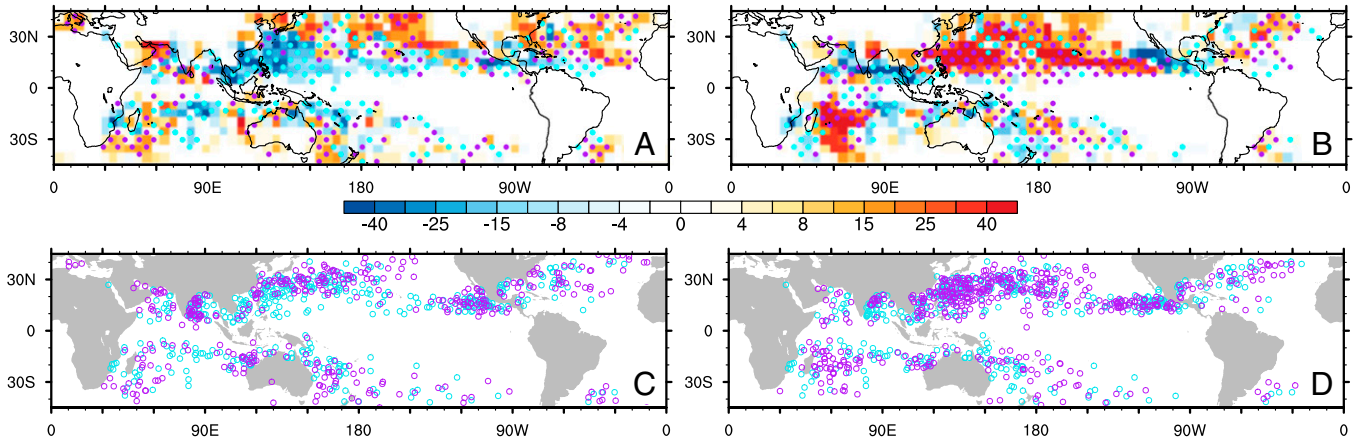

Fig. 2. Track/genesis density anomalies and location of peak intensity. Track density anomalies (shading) between the mid-Pliocene forced by the PRISM4/PlioMIP SSTs (*A* and *B*) and present-day experiments; units are cumulative 6 hourly storm position frequency per 5° × 5° gridbox in the last 5 y of simulations; positive and negative anomaly of cumulative genesis density is dotted in purple and cyan, respectively. Location of peak intensity in the present-day experiment (cyan circles) and in the mid-Pliocene experiments (purple circles) forced by the PRISM4 SSTs (*C*) and by the PlioMIP model-based SSTs (*D*).

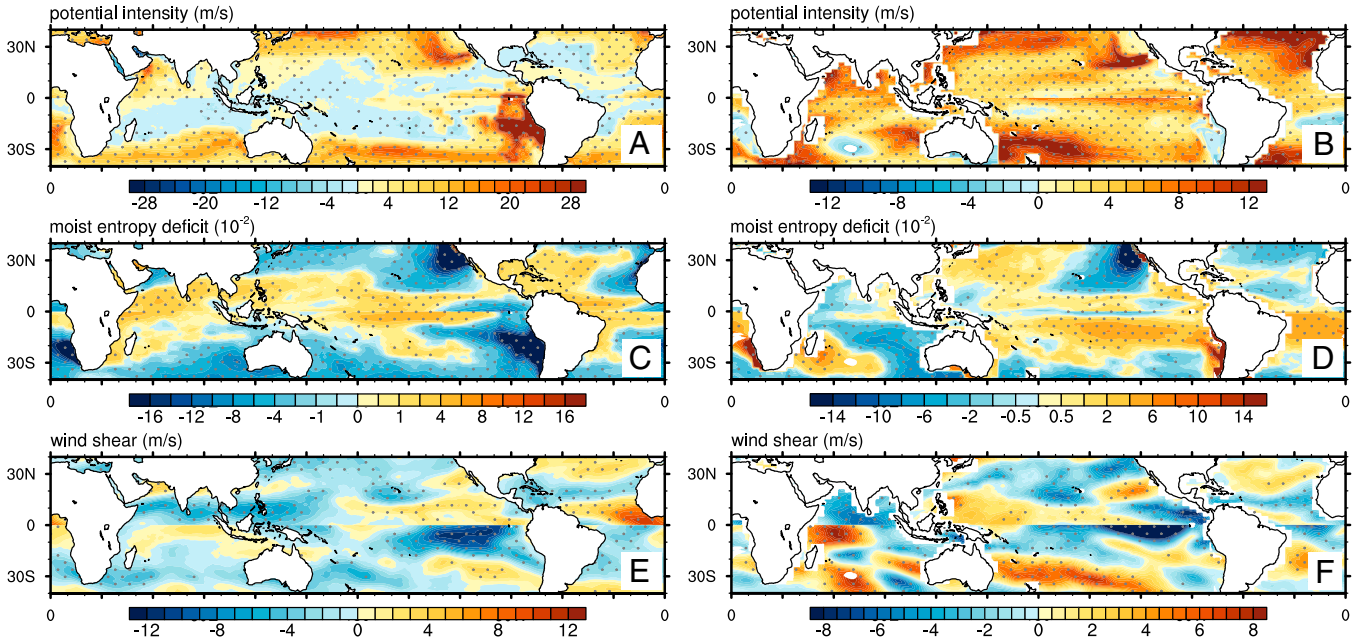

Fig. 3. Changes in storm season mean large-scale environmental conditions. (*Left*) Changes in potential intensity (*A*, meters per second), moist entropy deficit (*B*), and vertical wind shear anomalies (*C*, meters per second) between the mid-Pliocene experiment forced by the PRISM4 SSTs and preindustrial experiment. (*Right*) Same as *Left* but for anomalies between the mid-Pliocene experiment forced by the PlioMIP SSTs and preindustrial experiment. Storm season is defined as August–September–October in the Northern Hemisphere and January–February–March in the Southern Hemisphere. Areas passing the 90% significance test (two-tailed Student *t* test) are dotted.

However, changes in TC frequency differ with the imposed mid-Pliocene SSTs. CAM4 predicts a decrease of total TC number derived by the PRISM4 SSTs, whereas it gives an increase forced by the PlioMIP SSTs. This difference is mainly attributed to changes in TC frequency over the North Pacific, especially the number of the weakest storm system (Table S2). PDI is higher globally in both mid-Pliocene simulations, but it is enhanced over smaller parts of the central and eastern North Pacific in the experiment using the PRISM4 SSTs, whereas it is higher across the entire North Pacific in the simulation with the PlioMIP SSTs (Fig. S5). These differences in TC number and spatial patterns of PDI are largely caused by the discrepancy in temperature changes over tropical warm pool between the two mid-Pliocene SSTs (Fig. S6) and the associated changes in large-scale genesis factors (Fig. 3).

Power dissipation is related to the amount of wind energy available to mix the upper ocean, so the areas where enhanced TC-induced ocean mixing in the mid-Pliocene may occur in the North Pacific are sensitive to the SST pattern of the simulation. This result suggests that the condition of enhanced ocean mixing across the entire tropics in the early Pliocene (16) is dependent on the spatial pattern of SST anomalies. Given the current debate regarding stability of warm pool temperatures (14, 15, 23, 24), whether the TC feedback associated with ocean mixing is a potential factor for maintaining the reduced zonal SST gradient in the mid-Pliocene remains an open question.

As TCs are capable of causing substantial environmental, hydrological, and ecological disruptions, it is important to quantify and reduce uncertainty in model-based projections. The mid-Pliocene warm period offers an opportunity to better comprehend how TCs may vary in a warmer-than-present world. Our TC-resolving simulations consistently indicate that global-average TCs tend to become stronger, last longer, and migrate poleward, but there are caveats to be considered. The model resolution fails to capture storms of categories 3–5, which could affect the quantitative results reported here, as well as the modeled changes in the frequency of each TC category and distribution of PDI over individual ocean basins. However, this limitation may exert limited impact on the sign of TC metric change (Table 1) compared with results from a finer-resolution model that resolves intense storms, which has been proven true over the North Atlantic (25). In addition, the CAM4 model is forced with prescribed SSTs, which can lead to inaccuracies in the modeled potential intensity, as it is sensitive to the mechanisms that force SST variability (e.g., changes in surface winds versus shortwave or longwave radiation) (26). To better constrain TC activity during the mid-Pliocene and advance our understanding on future TC behavior, improved SST estimates in terms of accuracy and coverage and ultrahigh-resolution models (<10 km) are highly needed.

Methods

Climate Model. CAM4 is a global atmospheric model developed at the National Center for Atmospheric Research (27). CAM4 is coupled with the Community Land Model version 4 with prescribed SSTs. Here, CAM4 employs the finite-volume dynamical core and has a horizontal resolution of 0.23° latitude × 0.31° longitude (~25 km at the equator). The values of parameters and the subgrid-scale physical parameterizations are set to the default values at the standard resolution (i.e., 0.9° × 1.25°) without additional tuning.

Experimental Design. We design a preindustrial experiment and two mid-Pliocene experiments with prescribed SSTs using the CAM4 model (Table S3). In the preindustrial experiment, we use the default SSTs and sea-ice concentrations in CAM4, which is the monthly climatology during 1850–2010 based on HadISST1 and NOAA OI.v2 analysis (28). For greenhouse gases, we set the atmospheric CO_2 concentration to 280 parts per million by volume (ppmv), N_2O concentration to 270 parts per billion by volume (ppbv), and CH_4 concentration to 760 ppbv. Orbital parameters are set to the values of year 1950 and the solar constant is set to 1,365 W m^{-2}. Other boundary conditions (e.g., aerosols) are kept at the present-day levels.

In the standard mid-Pliocene experiment, the SSTs, topography, land cover, and CO_2 concentration are modified to represent the conditions of the mid-Pliocene based on the PRISM4 dataset (10). According to the guideline of the PlioMIP (29), we construct the SST fields and topography using the anomaly method. For example, we compute the SST difference between the mid-Pliocene and present derived from the PRISM4 dataset; these anomalies are transformed onto the CAM4 resolution and are then

added to the climatological monthly mean SST fields used in the preindustrial experiment. For the land cover, the reconstructed mid-Pliocene land cover is first converted to Land Surface Model land cover types and then to the plant functional types (30). The atmospheric CO_2 concentration increases to 405 ppmv. The other boundary conditions are identical to the preindustrial experiment.

Additionally, we perform a sensitivity mid-Pliocene experiment. The only difference between the sensitivity experiment and the standard mid-Pliocene experiment is that we construct the mid-Pliocene SSTs based on the ensemble mean of the PlioMIP models (13).

The atmosphere-only model adjusts to initial perturbation within several months, and high-resolution (i.e., 0.23°× 0.31°) simulations are quite time-consuming. Thus, the preindustrial experiment is integrated for 7 y and the two mid-Pliocene experiments for 10 years to reach quasi-equilibrium (Fig. S7). The last 5 y of results are analyzed in this study.

TC Tracking Algorithm. Detection of TCs from six hourly CAM4 model outputs is carried out using the Geophysical Fluid Dynamics Laboratory tracking algorithm (31, 32). Candidate TCs meeting the following conditions are located: (*i*) Local relative vorticity maximum (at 850 hPa) is larger than 1.6×10^{-4} s^{-1}; (*ii*) The closest local minimum in sea-level pressure that occurs within 2° of the vorticity maximum is defined as the storm center; (*iii*) The closest local maximum of 500–200 hPa mean temperature is defined as the warm-core center; (*iv*) The distance between warm-core center and the storm center is smaller than 2°, and the temperature decreases by at least 0.8 °C within a distance of 5° from the warm-core center.

Next, TC trajectories are calculated as follows: (*i*) Storms that occur within 400 km in the following 6 h are found; (*ii*) If only one storm appears within the 400-km region, it is defined as the same storm. If multiple storms are detected, the closest storm in the northwest quadrant (southwestern quadrant) of the Northern Hemisphere (Southern Hemisphere) is selected; (*iii*) a trajectory must last at least 2 d, with the maximum surface windspeed exceeding 17 m s^{-1} (not necessarily consecutive 2 d).

Large-Scale TC Genesis Factors. Potential intensity is a measure of the thermodynamic environment for TC genesis from soundings and a theoretical prediction of the maximum TC intensity (33):

$$PI = \sqrt{\frac{C_k}{C_d}\frac{SST}{T_o}\left(CAPE^* - CAPE^b\right)}, \quad [1]$$

where T_o is the mean outflow temperature, C_k is the exchange coefficient for entropy, C_d is a drag coefficient, $CAPE^*$ is the convective available potential energy (CAPE) of an air that has first been saturated at the temperature and pressure of the sea surface, and $CAPE^b$ is the CAPE of an ambient boundary layer parcel. Vertical wind shear generally inhibits TC genesis and intensification by shearing convective towers and ventilating the storm's core with subsaturated air (22). It is defined as the magnitude of the vector difference between the 200- and 850-hPa horizontal wind vectors. Moist entropy deficit is used to assess the moisture content of the middle troposphere (34):

$$\chi = \frac{s^* - s}{s_0^* - s^*}, \quad [2]$$

where s is a pressure-weighted mean of moist entropy over the free troposphere (850–200 hPa) and s_0^* and s^* is the saturation moist entropies of the sea surface and free troposphere, respectively. In general, higher potential intensity, smaller shear, and smaller moist entropy deficit each favors TC genesis and intensification, and vice versa. Increased potential intensity at higher latitudes, decreased potential intensity in the deep tropics, or both, could lead to a poleward migration of the location of peak intensity (5). A similar migration could be expected if wind shear/moist entropy deficit reduces at higher latitudes, wind shear/moist entropy deficit enhances in the deep tropics, or both.

ACKNOWLEDGMENTS. We thank the PRISM4 and PlioMIP groups for producing and making available their outputs. We thank the editor and two anonymous reviewers for helpful comments on an earlier draft of this manuscript, and we thank colleagues at the Nansen-Zhu International Research Centre and Climate Change Research Center for helpful discussions in preparing the manuscript. This study was funded by the National Natural Science Foundation of China (Grants 41402158, 41505068, and 41472160). R.L.K. is supported by National Science Foundation Grant AGS-1064013. J.P.K. is supported by National Oceanic and Atmospheric Administration's Center for Weather and Climate.

1. Christensen JH, et al. (2013) Climate phenomena and their relevance for future regional climate change. *Climate Change 2013: The Physical Science Basis. Contribution of Working Group I to the Fifth Assessment Report of the Intergovernmental Panel on Climate Change*, eds Stocker TF, et al. (Cambridge Univ Press, Cambridge, UK), pp 1248–1252.
2. Bindoff NL, et al. (2013) Detection and attribution of climate change: From global to regional. *Climate Change 2013: The Physical Science Basis. Contribution of Working Group I to the Fifth Assessment Report of the Intergovernmental Panel on Climate Change*, eds Stocker TF, et al. (Cambridge Univ Press, Cambridge, UK), pp 913–914.
3. Knutson TR, et al. (2010) Tropical cyclones and climate change. *Nat Geosci* 3(3): 157–163.
4. Kossin JP, Emanuel KA, Camargo SJ (2016) Past and projected changes in western North Pacific tropical cyclone exposure. *J Clim* 29(16):5725–5739.
5. Kossin JP, Emanuel KA, Vecchi GA (2014) The poleward migration of the location of tropical cyclone maximum intensity. *Nature* 509(7500):349–352.
6. Haywood AM, Dowsett HJ, Dolan AM (2016) Integrating geological archives and climate models for the mid-Pliocene warm period. *Nat Commun* 7:10646.
7. Dowsett H, et al. (1994) Joint investigations of the Middle Pliocene climate I: PRISM paleoenvironmental reconstructions. *Global Planet Change* 9(3):169–195.
8. Dowsett HJ, et al. (1999) Middle Pliocene paleoenvironmental reconstruction: PRISM2. US Geological Survey Open File Report 99-535 (United States Geological Survey, Reston, VA). Available at pubs.usgs.gov/of/1999/of99-535/. Accessed March 1, 2016.
9. Dowsett H, et al. (2010) The PRISM3D paleoenvironmental reconstruction. *Stratigraphy* 7(2-3):123–139.
10. Dowsett H, et al. (2016) The PRISM4 (mid-Piacenzian) palaeoenvironmental reconstruction. *Clim Past* 12:1519–1538.
11. Haywood AM, et al. (2011) Pliocene Model Intercomparison Project (PlioMIP): Experimental design and boundary conditions (Experiment 2). *Geosci Model Dev* 4(3):571–577.
12. Dowsett HJ, Robinson MM, Foley KM (2009) Pliocene three-dimensional global ocean temperature reconstruction. *Clim Past* 5(4):769–783.
13. Haywood AM, et al. (2013) Large-scale features of Pliocene climate: Results from the Pliocene Model Intercomparison Project. *Clim Past* 9(1):191–209.
14. Zhang YG, Pagani M, Liu Z (2014) A 12-million-year temperature history of the tropical Pacific Ocean. *Science* 344(6179):84–87.
15. O'Brien CL, et al. (2014) High sea surface temperatures in tropical warm pools during the Pliocene. *Nat Geosci* 7(8):606–611.
16. Fedorov AV, Brierley CM, Emanuel K (2010) Tropical cyclones and permanent El Niño in the early Pliocene epoch. *Nature* 463(7284):1066–1070.
17. Koh JH, Brierley CM (2015) Tropical cyclone genesis potential across palaeoclimates. *Clim Past* 11(10):1433–1451.
18. Knapp KR, Kruk MC, Levinson DH, Diamond HJ, Neumann CJ (2010) The International Best Track Archive for Climate Stewardship (IBTrACS). *Bull Am Meteorol Soc* 91(3):363–376.
19. Emanuel K (2005) Increasing destructiveness of tropical cyclones over the past 30 years. *Nature* 436(7051):686–688.
20. Kang N-Y, Elsner JB (2015) Trade-off between intensity and frequency of global tropical cyclones. *Nat Clim Chang* 5(7):661–664.
21. Holland G, Bruyère CL (2014) Recent intense hurricane response to global climate change. *Clim Dyn* 42(3):617–627.
22. Tang B, Emanuel K (2012) A ventilation index for tropical cyclones. *Bull Am Meteorol Soc* 93(12):1901–1912.
23. Ravelo AC, Lawrence KT, Fedorov A, Ford HL (2014) Comment on "A 12-million-year temperature history of the tropical Pacific Ocean." *Science* 346(6216):1467.
24. Fedorov AV, Burls NJ, Lawrence KT, Peterson LC (2015) Tightly linked zonal and meridional sea surface temperature gradients over the past five million years. *Nat Geosci* 8(12):975–980.
25. Knutson TR, et al. (2013) Dynamical downscaling projections of twenty-first-century Atlantic hurricane activity: CMIP3 and CMIP5 model-based scenarios. *J Clim* 26(17):6591–6617.
26. Emanuel K, Sobel A (2013) Response of tropical sea surface temperature, precipitation, and tropical cyclone-related variables to changes in global and local forcing. *J Adv Model Earth Syst* 5(2):447–458.
27. Neale R, et al. (2010) *Description of the NCAR Community Atmosphere Model (CAM 4.0). NCAR Technical Note NCAR/TN-464+STR* (National Center for Atmospheric Research, Boulder, CO), pp 1–188.
28. Hurrell JW, Hack JJ, Shea D, Caron JM, Rosinski J (2008) A new sea surface temperature and sea ice boundary dataset for the community atmosphere model. *J Clim* 21(19):5145–5153.
29. Haywood AM, et al. (2010) Pliocene Model Intercomparison Project (PlioMIP): Experimental design and boundary conditions (Experiment 1). *Geosci Model Dev* 3(1): 227–242.
30. Yan Q, Zhang ZS, Wang HJ, Gao YQ, Zheng WP (2012) Set-up and preliminary results of mid-Pliocene climate simulations with CAM3.1. *Geosci Model Dev* 5(2):289–297.
31. Knutson TR, Sirutis JJ, Garner ST, Vecchi GA, Held IM (2008) Simulated reduction in Atlantic hurricane frequency under twenty-first-century warming conditions. *Nat Geosci* 1(6):359–364.
32. Zhao M, Held IM, Lin S-J, Vecchi GA (2009) Simulations of global hurricane climatology, interannual variability, and response to global warming using a 50-km resolution GCM. *J Clim* 22(24):6653–6678.
33. Bister M, Emanuel KA (2002) Low frequency variability of tropical cyclone potential intensity 1. Interannual to interdecadal variability. *J Geophys Res* 107(D24):ACL 26-21–ACL 26-15.
34. Emanuel K, Sundararajan R, Williams J (2008) Hurricanes and global warming: Results from downscaling IPCC AR4 simulations. *Bull Am Meteorol Soc* 89(3):347–367.